THE ZEROING PROPERTIES OF QUARTZ WITH RESPECT TO DIFFERENT DEPOSITIONAL ENVIRONMENTS

Mark Android Rabin

Submitted in Partial Fulfillment of the Requirements
for the Degree of Bachelor of Science, Honours
Department of Earth Sciences
Dalhousie University, Halifax, Nova Scotia
April 2001

ABSTRACT

The zeroing of the luminescence signal in quartz grains by exposure to natural light is a key principle in sediment dating using optically stimulated luminescence (OSL) dating. Determination of the "equivalent dose", De, which is the consequence of a residual luminescence signal not completely erased by light in the natural environment, is expected to yield values close to zero. However, zeroing of surficial sediments has rarely been systematically tested for a range of modern settings. OSL works by evicting trapped electrons in the crystal lattice of a quartz grain by green light stimulation in 0.5 second exposure intervals resulting in a luminescence signal. Different depositional environments may allow incomplete zeroing by exposure to varying amounts of natural light, resulting in different OSL luminescence signals for each specific environment. The RAB-MB samples were taken from Martinique Beach, located on the Eastern Shore of Nova Scotia, and the HUD-2000-30A samples at depths of 29 m on the Scotian Shelf. Environments in question are lagoonal, beach dune, beach, and submarine sand dune. Using the single-aliquot regenerative-dose method De values of 2.053 ± 0.308 Gy (natural irradiation) and 0.430 ± 0.517 Gy (irradiated with 3 Gy of beta radiation) were acquired for RAB-MB-1, collected under shallow water in a back-barrier lagoon.. Due to time constraints, only one sample could be tested. The latter of the two De values suggests that with a suitable lab protocol, more accurate De values can be obtained. Although the standard deviation is high, the second De value satisfies an accurate zeroing of quartz grains in the lagoon environment.

Key Words: OSL dating, zeroing, Martinique Beach, single-aliquot

ACKNOWLEDGEMENTS

This thesis would not have been completed without the encouragement and assistance of Kevin Vaughan and Pat Scallion. I would like to thank the sympathetic and understanding Dr. Martin Gibling for taking time from his busy day to talk about thesis difficulties and review rough drafts. In the last few days of the final draft, Dr. Peter Reynolds has gratefully lent his expertise to data analysis. I would also like to recognize the efforts of Dr. Dorothy Godfrey-Smith, whom without, I would not be doing this thesis. And I finally I would like to thank my geo-pal Mark C. Coakley for endlessly complaining with me about thesis issues.

TABLE OF CONTENTS

LIST OF FIGURES

LIST OF TABLES

CHAPTER 1: INTRODUCTION

1.1 Statement of Purpose

The purpose of this thesis is to investigate a very important variable in the absolute dating of quartz-bearing sediments using optical dating. The variable under consideration is the zeroing of the luminescence signal in quartz grains by exposure to natural light. Optical dating uses a technique that evicts trapped electrons from imperfections in the crystal lattice or traps and measures their intensity in the form of a luminescence signal. Electrons are cleared from these traps by exposure to sunlight and the quartz grains are said to be "zeroed" or the luminescence clock reset. The luminescence clock begins counting when there is no longer any exposure to natural light. Therefore, the total amount of sunlight that each grain receives is likely to vary with respect to different means of transportation and depositional environments. Different depositional environments dictate how much sunlight bulk sediment and specifically a grain of quartz will experience. The more frequent and longer the exposure to sunlight, the more complete the zeroing of the luminescence signal in the grain. In studying the completeness of zeroing in quartz grains, hopefully, a correlation with specific depositional environments can be made. If so, we can estimate a residual luminescence signal for each depositional environment investigated. This will enable us to apply a residual luminescence correction to old sedimentary deposits created in the

same depositional contexts as the modern analogues we have studied.

This thesis will centre on determining the "equivalent dose", D_e, which is the consequence of a residual luminescence signal not completely erased by light in the natural environment, from modern sediments. The specific environments investigated in this study are beach (summer to winter), beach dune, lagoon, and submarine sand dunes.

1.2 Interest in Studying Zero Age Modern Sediment

In order to understand and date older sedimentary deposits using the optically stimulated luminescence (OSL) method, an understanding of modern sediment travel and how young (zeroed) they are is needed. Optically stimulated luminescence is used to date young, unconsolidated sediments. Through OSL dating, a greater understanding of modern sedimentary environments and grain motions in bulk sedimentary transport is acquired. Studying zero age modern sediments can help in determining: 1) Processes of deposition - whether the grains were suspended for a long time or directly deposited and buried, what type of sedimentary structures are formed instantly or over a period of time; 2) Erosion from pre-existing deposits; 3) Transportation- was it a turbulent or laminar flow, long or short distances, velocity of the medium; and 4) Reworking of modern sediments.

1.3 Sediments: Deposits, Sedimentary Processes, Rates of Transportation, Deposition, and Burial

In order to understand the luminescence properties of quartz grains, depositional properties of sediments have to be understood. Each depositional environment differs in terms of sediment transport and deposition. In order for the sediment to move, it needs a medium strong enough to entrain the grains. The main transport media for sediments are water, air, and ice. An important factor in the study of sediments is place of origin. If there is a large granitic body near by, it is most likely that the sediments were derived from this location. Depositional environments, observed in this thesis and found all over the world, are aeolian, beach, lagoonal, and oceanic.

1.3.1 Beach

Beaches are areas of sediment accumulation that are affected by waves breaking on the coast. Beaches are continually being reworked by the back and forth wave action, which can range in force from gentle to very strong (a storm for example). The sediments on beaches are generally made up of clastic or carbonate material, and most of the time both types are present. These sediments are moved back and forth along the beach, causing the clasts to become well-rounded and well sorted. In order for sediment to be accumulated on a beach, a source of sediment is needed. If this is not present, the beach can not replenish itself and tends to be small with large clasts that cannot be easily moved by wave action. Beaches that have low-angle stratification, and sediments that are

well sorted and rounded, are characteristic of a wave-dominated environment (Nichols 1999).

Beaches are continually changing, although they appear to remain the same. This is a result of a beach equilibrium that has to do with the type of wave action present. A summer beach will tend to accumulate sediment due to the gentle waves, bringing in similar or greater amounts of sediment than is being removed. On the other hand, a winter beach is usually rocky and bare, as a result of large storm waves that reach far up the beach and remove more sediment than is being brought in (Duxbury and Duxbury 1997). The arrival of more sediment in the spring, can be a result of river flooding and winter melt, the shoreward currents carrying sediments stored offshore, and much gentler beach system.

Waves generally approach at an angle to the beach, creating a longshore current. Thus, sediment suspended by wave action in the surf zone (water depth ~ 1-2 metres) undergoes longshore transport along the beach. The up-rush or swash, of water from each breaking wave moves the sand particles diagonally up and along the beach in the direction of the longshore current. Combined with the backwash action, water moving back down the beach towards the water, the sediments move in a zigzag or sawtooth path along the swash zone of the beach as part of the longshore transport (Duxbury and Duxbury 1997).

1.3.2 Aeolian-beach dunes

Aeolian or desert type sediments are a group that are not regularly affected by water as a main form of sediment movement. Deserts are characterized by sparse vegetation and low rainfall. The majority of the sediment is found as sand in well sorted aeolian dunes, poorly sorted conglomerate (as a result of flash floods) on alluvial fans, mud in some desert rivers and evaporite minerals (Nichols 1999). Because the optical dating method uses quartz, most of the OSL samples tend to be taken from the well sorted aeolian dunes. Particle movement in the aeolian environment is mainly by air. Wind transport can be observed on dry beaches and the sediments collect as a dune at the back of the beach.

In aeolian transport, high wind velocities are needed in order to achieve sufficient force to move sand particles. This is due to the low viscosity of air compared to that of water, therefore causing a large density contrast between air and sediments. Coarser sand particles cannot be carried by wind, resulting in only fine to medium sized sand being readily moved into the air and around the desert. Rolling, saltation, and suspension of grains are observed in air transport (Prothero and Schwab 1996).

Characteristic deposition of aeolian sediments is mainly in the form of ripples and on a larger scale, dunes. These bedforms are similar to ripples and dunes found in subaqueous environments. Enormous cross-beds, which are generally associated with aeolian dunes and ripple marks are preserved in the geologic record. The scale of these dunes is proportional to the strength of the wind (Nichols 1999). The stronger the wind, the larger the dunes.

Beach dunes are a result of onshore winds that transport sediments from the beach into the back-berm of the beach resulting in an aeolian dune (Duxbury and Duxbury 1997). These dunes are parallel to the coast, and can extend from a few metres to kilometres inland. The process of transport and deposition is the same as desert dunes, although vegetation is likely to be present and will stabilize the dune and disrupt dune cross-bedding.

1.3.3 Lagoon

Lagoons are areas of quiet conditions and low-energy sedimentation, generally found behind beaches and beach dunes. Small waves may form on the surface of these permanent bodies of water. Sediment that is moving through tidal inlets tends to be deposited as flood-tide deltas. Along with the organic clays, fine sediment from the beach may blow over into the lagoon, this is often referred to as "washover" (Nichols 1999).

1.3.4 Submarine Dunes

Submarine dunes form quite similarly to aeolian dunes, except sediment is displaced by underwater currents instead of wind. They display cross-bedding, and sediment grains undergo rolling, saltation and suspension. Major storm activity can also affect dune movement.

1.4 Sedimentary Environments in Terms of Rates of Light Exposure and Net Light Exposure

As sediments travel from their place of origin to their place of deposition and eventual burial, they undergo exposure to sunlight. The amount of sunlight that a grain of quartz takes in prior to burial is dependent on the environmental circumstances (Huntley and Lian 1997). Therefore, each depositional environment, on a general basis, should yield characteristic sunlight intake properties. The total effective light exposure of a grain is a function of many variables that work together or individually.

1) Velocity and mode of transport – The speed of the transport medium will affect sediment exposure to light. Suspended sediment has a greater probability of being exposed to sunlight. Slower moving fluids tend to have less suspended sediment than faster, turbulent media. The faster the velocity, the larger the spectrum of grain sizes and types. The higher up the sediment is in the water/air column the greater the chance of exposure to sunlight.

2) Grain size – The size of the grain will dictate whether it will stay in suspension, or fall to the bottom of a water or air column. Finer grains tend to stay in suspension, therefore increasing their exposure to sunlight, whereas coarser, saltating grains undergo less light exposure.

3) Distance – The farther the grain travels, the more opportunity it has to be exposed to light.

4) Amount of reworking/recycling – The more reworking and recycling that a

grain undergoes, the longer the grain will remain active, therefore increasing its exposure to sunlight.

5) Filtering of sunlight - Sunlight that penetrates the water column is affected by the depth and amount of suspended sediments. Light will have difficulty reaching grains in water with large amounts of suspended sediment. As depth increases, light decreases, therefore the spectrum of light is altered by water (Berger 1990)

6) Seasonality and daytime hours – Sediment travelling in a mid-summer water environment may display calm and somewhat clear conditions, whereas that same body of water in the spring may be turbid and fast paced. In the summer months, the days are longer, allowing more time for light exposure to sediments. Sediment that is buried/transported at night may not be exposed to any type of light, and therefore not be properly zeroed.

Rate of light exposure is a function of rate of transportation plus sediment density in current flow. Net light exposure is a function of rate of light exposure during transportation plus speed of burial after deposition.

The beach environment provides a potentially good sunlight exposure medium. As indicated earlier, sand on a fairly gentle beach gets moved back and forth between the water and the beach. When sediment transportation occurs, the grains are usually suspended in the first couple of meters of water and/or by the wind, allowing for consistent exposure to sunlight in both circumstances. Before sand on a beach is finally deposited into the sediment record, it is possible for a grain to have been moved around

and exposed to sunlight for a prolonged amount of time (~ couple of months) with only temporary stoppages.

The aeolian environment demonstrates some of the best potential sedimentary functions in terms of light exposure. The grains are not suspended in water, therefore taking in the sunlight directly. When the grains are transported, they are brought up into the air exposing them even more directly to the sun. Upon deposition, they are again exposed to direct sunlight until they are covered up.

The lagoonal environment, with its slow moving, shallow water and low-depositional rate, in theory appears to be have the potential of an area of maximum light exposure. It is possible that organic growth and mud suspension could block off large amounts of light to sand grains.

Submarine dune environment, depending on the suspension of particles in the water, and depth of the submarine floor, can either be well exposed or underexposed to light.

For the purpose of this thesis, the particular sediment samples were selected to be able to compare and contrast sedimentary environments in terms of exposure to natural light as a result of different sediment variables. For example, a comparison between sand dune vs. submarine dune will give an indication of the filtering function in water.

CHAPTER 2: OPTICAL DATING AND THE ZEROING PROCESS/METHODS

2.1 Optical Dating Overview

Optical dating (optically stimulated luminescence or OSL dating) is a technique whereby the amount of time elapsed since a sediment was buried can be determined. Measurement of this property is dependent on the amount and type of exposure to natural sunlight, which can vary from direct sunlight, to overcast and submarine conditions. As seen in Chapter 1, there are many variables in the depositional environment that affect the amount and intensity of sediment exposure to light. Exposure to natural light is the key factor in OSL dating.

OSL dating was developed by Huntley et al. (1985) at Simon Fraser University in Vancouver, Canada. Optical dating generally uses quartz and feldspar grains for dating and comparison due to their widespread availability and luminescence properties. For the purpose of this thesis, quartz grains are observed. Upon exposure to sunlight, electrons stored in light-sensitive traps are evicted, effectively 'bleaching' or 'zeroing' the previously acquired luminescence signal in the quartz grain (Aitken 1985; Huntley and Lian 1997; Murray and Olley 1999). These traps are found as imperfections in the crystal lattice where energy, in the form of electrons, can be stored and accumulated for long periods of time (section 2.2). Electrons begin to accumulate in these traps as soon as exposure to light has ceased, and the sediment has been plunged into darkness.

OSL dating works by measuring the intensity of the luminescence signal that is given off when grains are subjected to initial exposure to light. Light that is initially shone on the quartz and the light that is emitted are assumed to be a stream of photons, where the incident beam has a small range of energies compared to the emitted beam which displays a large spectrum of energies (Huntley and Lian 1997). The more intense the luminescence signal, the greater the amount of electrons trapped in the grain. Understandably, a sample that has recently been well exposed to sunlight (or artificial light) will result in the release of very few to no electrons and therefore a very low emitted photon beam.

Determining the age of last exposure to natural light encompasses many factors, but the general equation is

$$\text{Age} = \frac{\text{Equivalent Dose (De)}}{\text{Dose Rate}}$$

Determination of the equivalent dose, De, is done by measuring the energy stored within the grains, when they are exposed to a calibrated ionizing-radiation source in the laboratory (Murray and Olley 1999). The most common method is a radioactive source emitting gamma rays or beta particles (Murray and Olley 1999). Although there are complications due to past exposure, the main focus is to find out the amount of natural radiation that was absorbed from the most recent exposure to light, giving us the equivalent dose. This is achieved by measuring the luminescence signal that represents

the natural dose, then irradiating the sample, or subjecting the sample to a known dose of radiation and measuring its response. Samples and protocols usually fall into two broad categories: single-aliquot and multiple-aliquot.

The multiple-aliquot additive dose method, one of the earliest techniques, uses 2 to 100 sub-samples (aliquots) all sharing identical characteristics. In this method, aliquots are separated from the sample and given different laboratory doses in addition to the natural dose. The samples are then heated and the luminescence signal measured. The signals are then plotted on a luminescence intensity vs. laboratory dose graph and a line is fitted, which is then extrapolated to zero intensity where the dose intercept is taken to be the equivalent dose, De (Huntley and Lian 1997). The heating process is required to compensate for thermally-activated processes that would have affected the buried sample and are not effective in the lab. As a result of solar resetting, it should be understood that not all the grains in the sample have been equally represented. This can cause some potential problems, but much effort has been put into modification of multiple-aliquot methods in order to compensate for this.

The single-aliquot regenerative-dose method outlined in Murray and Olley (1999), is a more recent development and a significant improvement in luminescence technology. Using this method, a natural aliquot is subject to a preheat (10s at ~240 °C) and then undergoes a brief light exposure from which an OSL signal is released, measured and a laboratory dose given. The aliquot then undergoes an additional preheating and a brief light exposure, and again the OSL signal is measured and a new laboratory dose given. This process is repeated several times, resulting in increasing

OSL signals. These OSL signals are underestimates of the accurate response because i) with each exposure to light, the trapped electron population decreases, and ii) each time the sample is preheated, a small fraction of electrons are thermally activated and released from their traps. To make up for this cumulative loss, a correction has to be applied and is achieved by continuing the preheat and stimulation cycle on the same aliquot, although no more doses are added. The observed OSL signal consistently decreases. The single-aliquot method has proven to yield better results because many samples can be compared rather than generating one average of multiple-aliquots. The single-aliquot method still has its limitations due to the fact that the equivalent dose, De, has to be extrapolated.

The regeneration method exposes aliquots to laboratory light (sunlight or artificial) in order to empty the traps or remove the OSL signal and then the signal is regenerated by laboratory radiation doses. The natural dose is also measured. This methods works under the assumption that by bleaching the sample, it is restored to its condition immediately after burial, and the exact amount of radiation needed to equal the natural dose can be calculated. By using this method, sensitivity changes are introduced. These be corrected by measuring the sensitivities that where applied in the measurement of the natural signal, and applying them to the regenerated OSL signal.

The dose rate of a sediment is a function of the radioactive decay of potassium, ^{40}K, uranium, ^{238}U, thorium, ^{232}Th, and rubidium, ^{228}Ra and their decay products, found in the grain and in the sediments that border it (Huntley and Lian 1997). Cosmic rays also contribute to the dose rate. The dose rate is reduced by the absorption of energy by water in the sample. Involved in the determination of the dose rate, the radionuclide

concentrations need to be measured in the sediment by gamma spectrometry, as does the average water content over the duration of the deposit and the dose rate from cosmic radiation.

2.1.2. Advantages of Single Aliquot analyses:

When optical dating was first invented, all De measurements were performed using additive dose growth, prolonged optical stimulation of up to 250s, and multiple aliquots at each dose. With this approach, all aliquots contributed to a single, multi-point growth curve, from which a single De was deduced.

On the other hand, single aliquot analysis permits a De to be deduced for each individual aliquot, independently of all others. This way, typically 10 to 20 independent De estimates may be obtained for each sample. An average of these De's is expected to be the same as the single De obtained using the multiple-aliquot method.

An additional advantage exists for single aliquot analyses, however, which consists of being able to examine the distribution of De's in order to determine the degree to which the sample is "well behaved". The meaning of this is best explained through illustration, using recently obtained data from a set of samples in South Carolina, USA (D.I. Godfrey-Smith and A. Ivester, personal communication).

In the sample SC3 below, 10 aliquots were measured. All yielded a similar De, which is pooled to yield an average De = 14.8 ± 0.9 Gy. The fact that there is no

dependence of each De with the initial luminescence of that De's aliquot indicates that all grains in this sample were completely zeroed upon deposition, and that the sample remained undisturbed during burial.

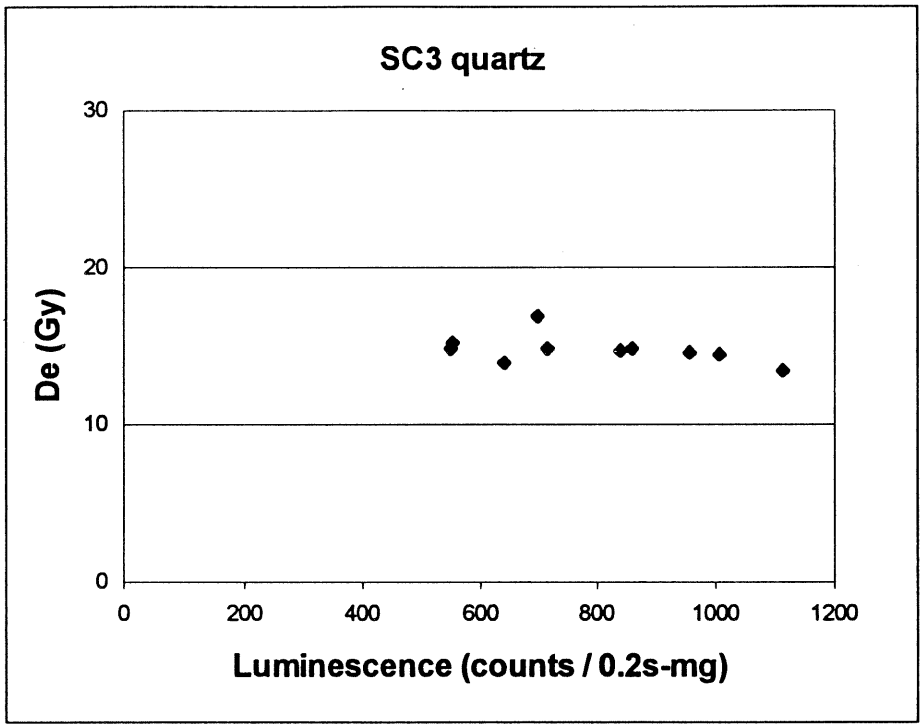

Figure 2.1 – Demo graph from recent South Carolina sample 3

Sample SC7 below has a different De-luminescence distribution. As well as a cluster of 6 aliquots with very similar De and luminescence properties, three aliquots clearly are outliers. While the cluster yields a good average De of 23.8 ± 1.8 Gy, the full set yields a De of 24.9 ± 4.3 Gy and an unacceptably large standard deviation. It is possible that the outliers are due to incompletely removed contaminants such as feldspar or zircon grains, or to grains from adjacent stratigraphic units incorporated into this

sample through in situ biological activity (burrowing animals, plant roots). Their "outlier" status would not be easily recognized in a multiple aliquot growth curve, which would therefore yield a poor De.

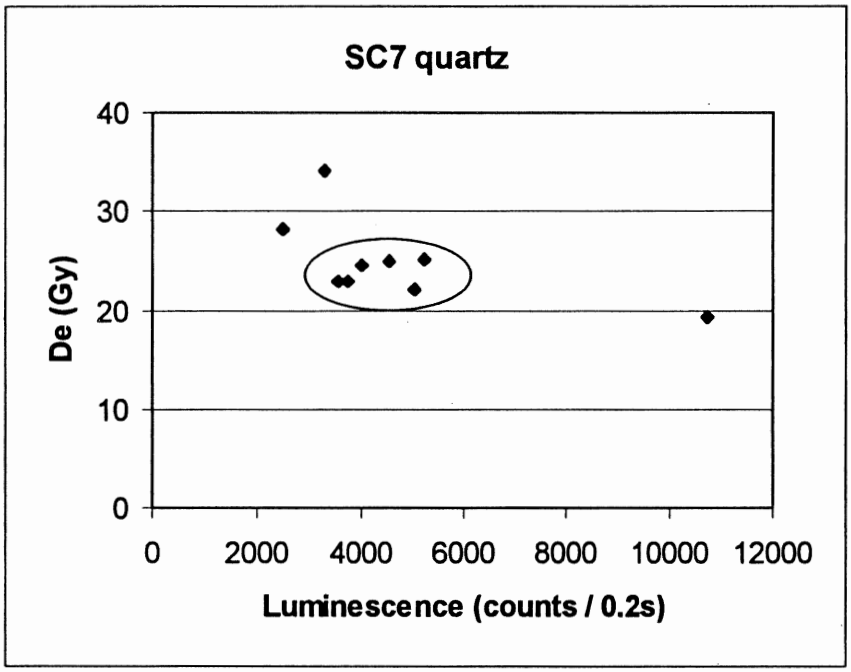

Figure 2.2 – Demo graph from recent South Carolina sample 7

The sample SC12 is a modern surface sample. It was created by modern deflation processes of adjacent strata. The De-luminescence distribution shows a striking correlation of the two variables. This indicates that not all grains in this sample experienced the same degree of bleaching; the less completely bleached aliquots yield a higher De, as expected. Although these aliquots yield an average De of 0.039 ± 0.023 Gy, the minimum De of 0.04 Gy reflects the residual luminescence of the most

completely bleached grains.

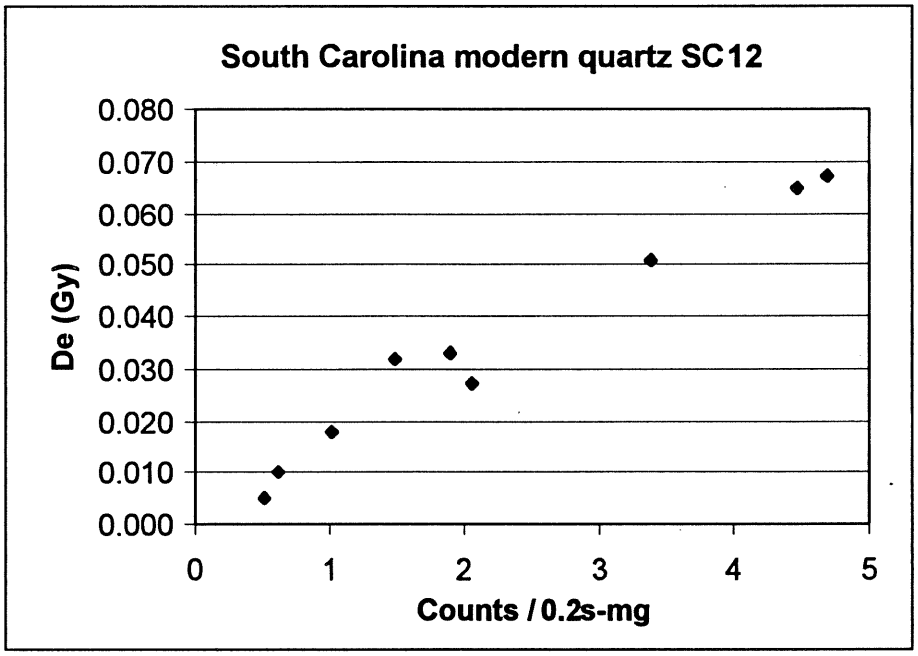

Figure 2.3 – Demo graph from recent South Carolina sample 12

2.2 Age Range

Using the formula outlined in section 2.1, an age since last exposure to light can be found. The general age range that has been achieved is from about 1000 years to 100,000 years (Huntley and Lian 1997). With meticulous lab work, and grains that were consistently well exposed to light, ages of 100 years or less can be achieved. Ages in the order of one year to over 1,000,000 years have been achieved, but no reliable technique exists to consistently obtain these results. For the purpose of this thesis, modern age

sediments are being tested, and should yield very low ages, with equivalent doses, D_e, being close to zero. In order to attain accurate ages, sediments must have undergone complete resetting or zeroing, this being one of the main determinants in age accuracy. The ages can also be affected by past histories of the sample in question and whether or not the grain has been completely zeroed (see section 2.4 on incomplete zeroing).

2.3 Types of Sedimentary Deposits that are Dateable in Terms of Exposure to Light

The optical dating method can be used to date sediments, from almost any depositional environment as long as there is exposure to natural light and quartz and feldspar are present. Optical dating was first used to date deep-sea sediments but has since been used to date aeolian, fluvial, glacio-fluvial, marine sediments, and even slope wash and colluvium (Murray and Olley 1999). Aeolian sediments tend to display the most reliable ages, due to the nature of aeolian transport (see section 1.3) and its effectiveness in resetting the OSL signal. In the case of fluvial and colluvial sediments, exposure to light can vary due to the turbulent nature of sediment transport, and will vary from grain to grain.

2.4 Possibilities of Incomplete Zeroing and Implications for Dating of Very Young Deposits

One of the most important aspects of OSL dating is how much exposure to sunlight a deposit undergoes before burial, which is directly related to complete, fully zeroed or reset, or incomplete zeroing of the sediment. Many problems in optical dating arise from incomplete resetting of the luminescence signal, which causes overestimations in sediment ages (Aitken 1985; Huntley and Lian 1997; Murray and Olley 1999). Incomplete zeroing of a sediment will result in an age corresponding to an earlier exposure event in the sediment's history. As a general rule of thumb, most sedimentary deposits, even aeolian, display a heterogeneous OSL signal which means that when the signal of a large number of grains is averaged, it results in an overestimated age. The degree to which sediment is zeroed, which depends on sufficient exposure to sunlight, is directly related to the type of sediment transport and whether this allows sufficient grain exposure to light. Having a good grasp of the sedimentary process that affect the samples will help in determining if the age estimation is accurate or not. The lower the equivalent dose, the closer its true burial age will be.

CHAPTER 3: SAMPLES AND INFORMATION

3.1 Martinique Beach & Lagoon

Martinique Beach, is a white, sandy beach located on the Eastern Shore of Nova Scotia (Fig. 3.1) and is about 5 km in length.

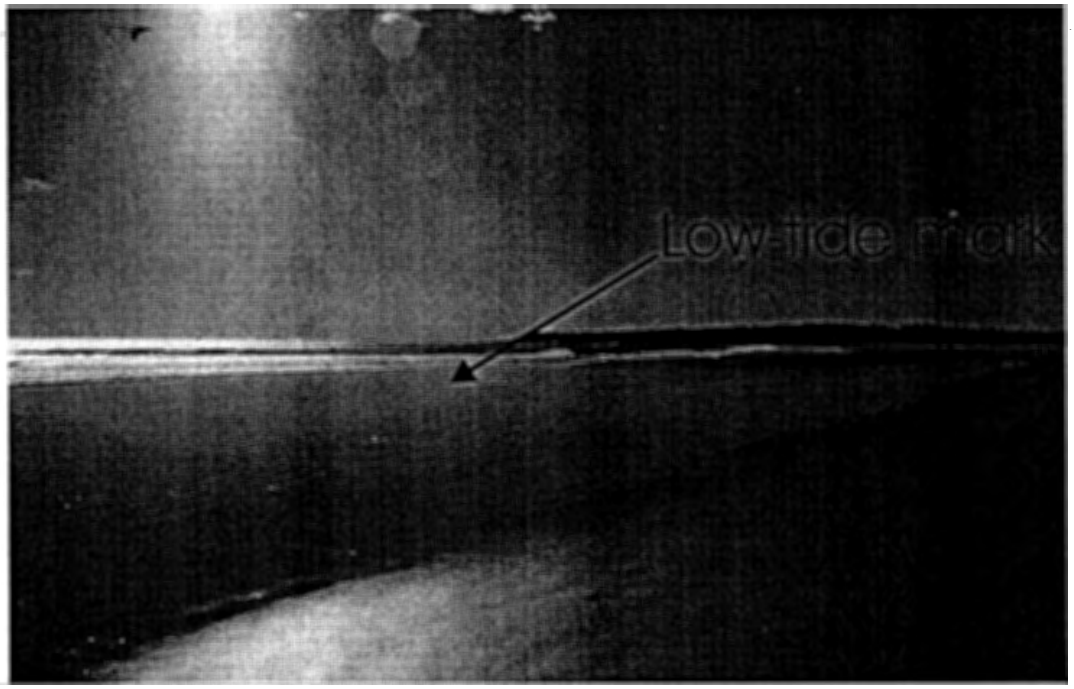

Figure 3.2 - Low tide at Martinique Beach

On September 29, 2000, six samples were taken from a range of locations along Martinique Beach and lagoon at low tide. Samples RAB-MB-1,2, and 3, were placed

Figure 3.1 - Map of Nova Scotia with inset of Martinique Beach

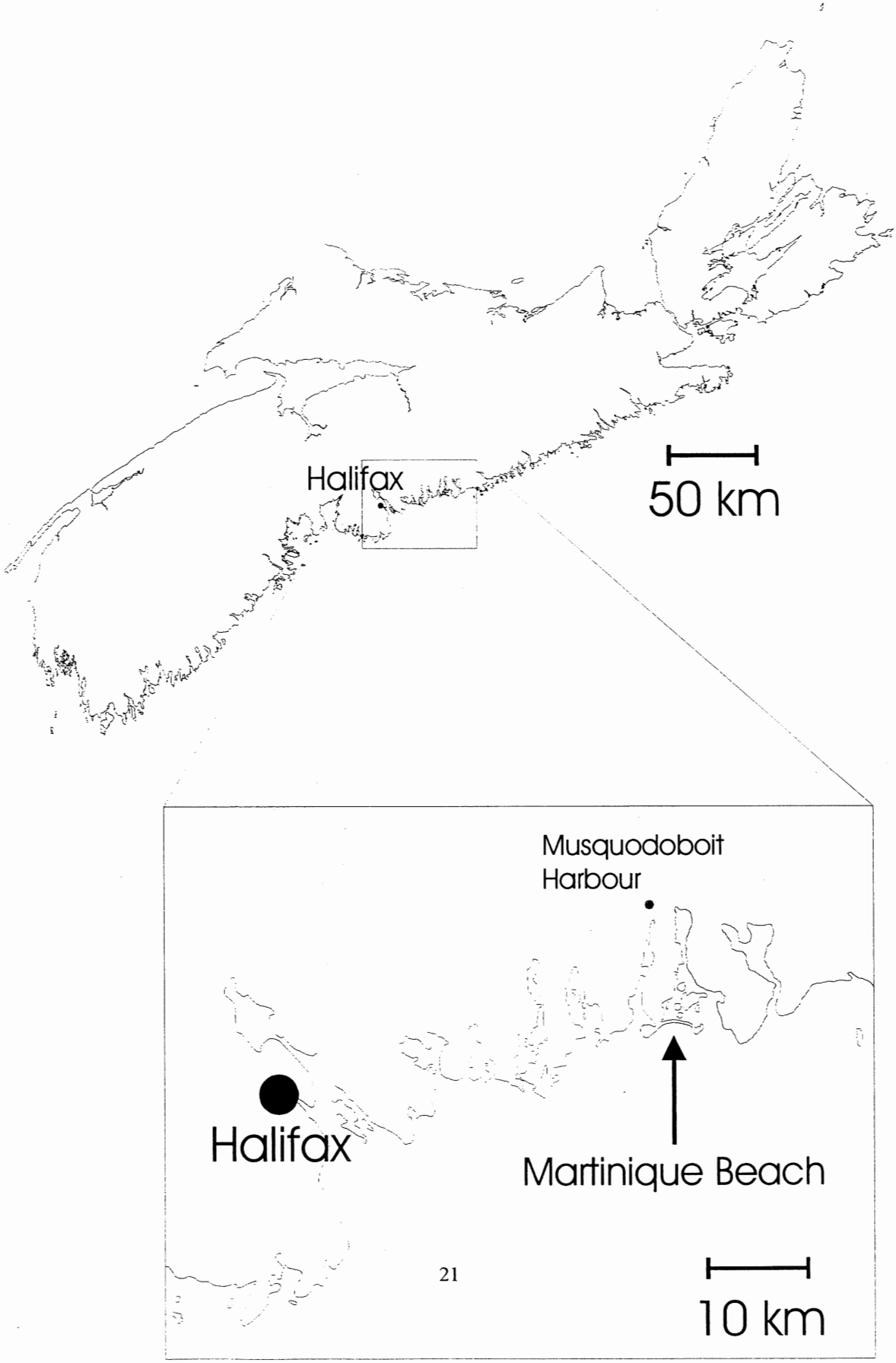

directly into tin cans and sealed as they appeared at the surface, therefore they were continually exposed to light until collected. Samples RAB-MB-4 and 5 were collected by pushing the tin cans into the side cut, therefore the samples remained in darkness, and were sealed. Sample RAB-MB-6 was taken from the bottom of the dug out hole (see RAB-MB-6) and loosely shoveled into the tin can. A schematic cross-section of Martinique beach and sampling area is shown below.

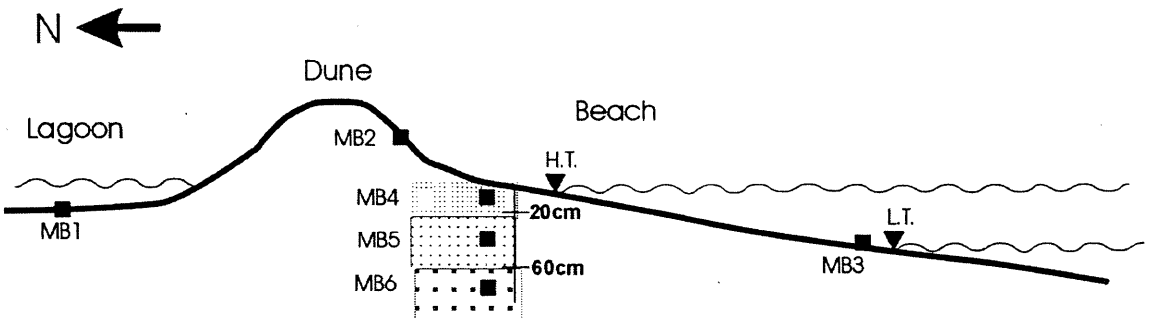

Figure 3.3 - Schematic of Martinique Beach, showing the relationships between the samples collected. The MB4 to MB6 area is stippled to indicate the textural differences of the sand in the section. Distances not to scale. HT = high tide, LT = low tide.

RAB-MB-1

This sample was taken from the lagoon behind the beach, approximately 25 m into the center of the lagoon (Fig 3.4). Taken from the top 4 cm, the sample was mainly dark silty sand with organics intermingled, with a clay film on top. The structural appearance of the lagoon seemed hummocky with water puddles spread unevenly in the troughs.

RAB-MB-2

Sample 2 was collected from the dune at the back of the beach (Fig. 3.5). The sample was taken on the lee side of the dune, about 0.5-1 m below the crest, and 1.5 m from the beach, at the start of vegetation. Collected from the top 1 cm, the sample is almost entirely composed of well sorted, fine, dry sand.

RAB-MB-3

Sample 3 was collected in the intertidal zone, near the low-tide mark. The top 0.5 cm of the beach was sampled (see Figure 3.2).

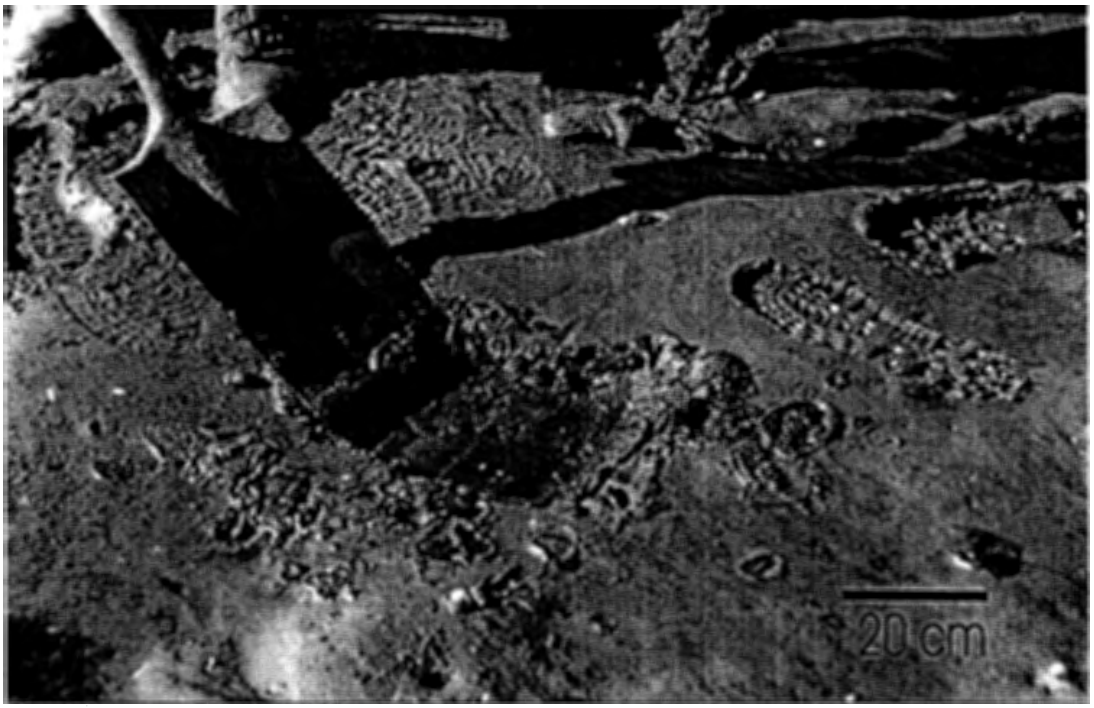

Figure 3.4 - Back lagoon, Martinique Beach, sample RAB-MB-1

Figure 3.5 - Back dune, site of sample RAB-MB-2

The next 3 samples have been taken from a hole dug in the beach, approx. 10 m from the dune vegetation and 80 cm in depth. Three distinct layers were present from top to base: Layer 1- fine laminated sand and silt, 0-20 cm (Figure 3.6); layer 2- medium to coarse sand coarsening downwards with some apparent cyclicity, 20-60 cm, and a very clear demarcation between fine and coarse sand at 40 cm (Figure 3.6); and layer 3- the basal part of the pit was composed of very coarse sand with gravel and pebbles, 60+ cm.

RAB-MB-4

Sample 4 is made up of well sorted, fine sand and silt, taken in layer 1 (Figure 3.7), 12 cm below the top of the beach.

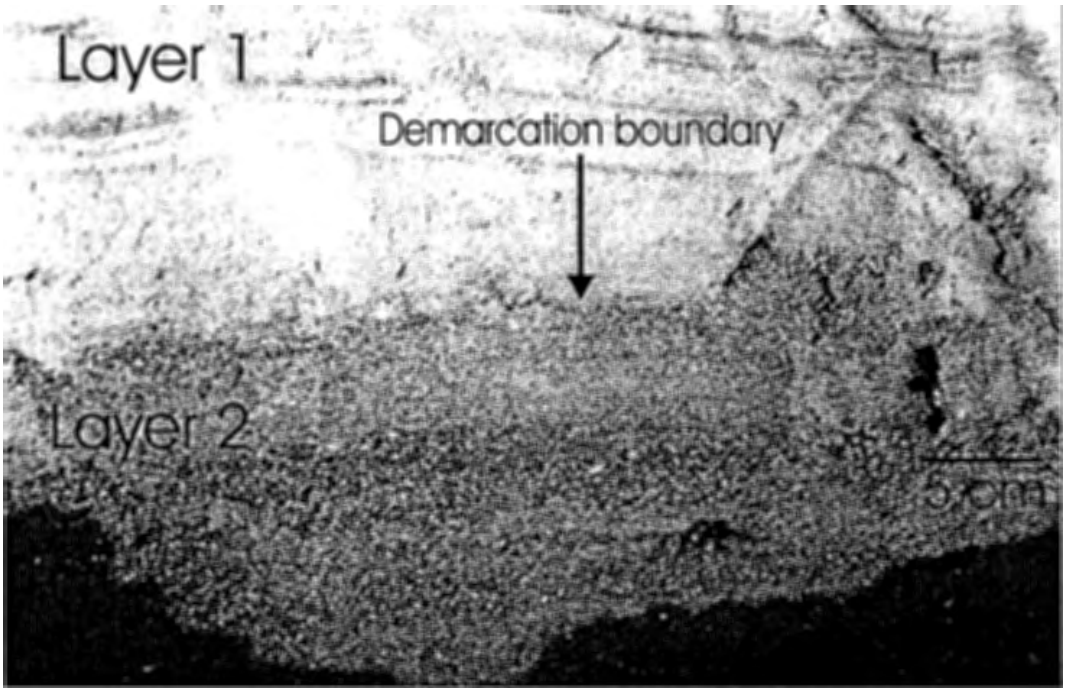

Figure 3.6 - Demarcation boundary between layer 1 and layer 2.

RAB-MB-5

Sample 5 is made up of coarse sand with small shell fragments. This sample was taken 45 cm below the top in layer 2.

RAB-MB-6

Sample 6 was taken from the bottom of the pit, and is made up of beach gravel of pebble size, shell fragments, coarse grained sand, and fine grained sand

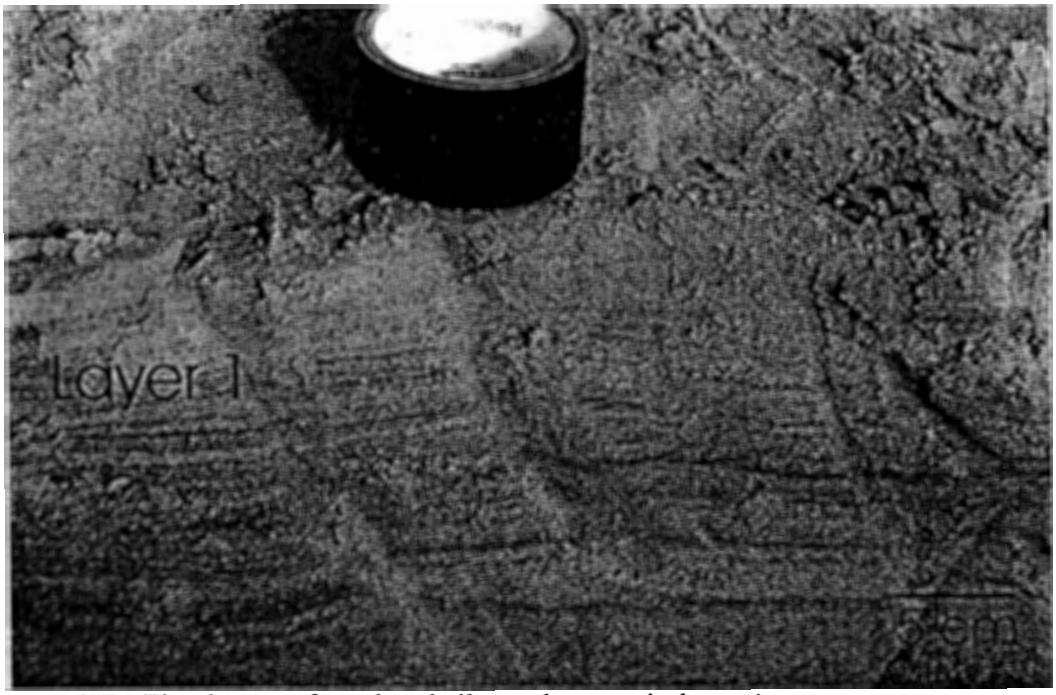

Figure 3.7 - Fine layers of sand and silt can be seen in layer 1.

3.2 Sable Island submarine sand dunes

Samples HUD 2000-30A-62, HUD 2000-30A-63, and HUD 2000-30A166b were collected from July 13-21, 2000 on the Bedford Institute of Oceanography (BIO) sponsored cruise of the Hudson scientific research vessel on the Scotian Shelf. These samples are almost entirely made up of well sorted quartz grains. In order to avoid light contamination, the cores were initially opened and observed under subdued red light at BIO. The samples were scooped into light-tight metal containers and transported to the OSL lab at Dalhousie University. (For sample locations on the Scotian Shelf, see Table 3.1 and Figure 3.8)

HUD 2000-30A-62

This core was taken at a water depth of 29 m .The sample was taken from the upper 4-9 cm of the core.

HUD 2000-30A-63

This core was taken at a water depth of 26 m. The sample was taken from the upper 7-12 cm of the core.

HUD 2000-30A166b

This core was taken at a water depth of 29 m. The sample was taken from the upper 5-10 cm of the core.

Table 3.1 - HUD-2000-30A sample information
(King, E., unpublished, 2001)

STATION NUMBER	LATITUDE	LONGITUDE	CORE LENGTH	WATER DEPTH (m)	GEOGRAPHIC LOCATION
62	43.941943	-60.559575	112 cm	29	Scotian Shelf - Sable Island Bank - COPAN-1 Site
63	43.933163	-60.547413	55 cm	26	Scotian Shelf - Sable Island Bank - COPAN-1 Site
166	43.899081	-60.087558	199 cm	29	Scotian Shelf - Sable Island Bank - South Sable Island

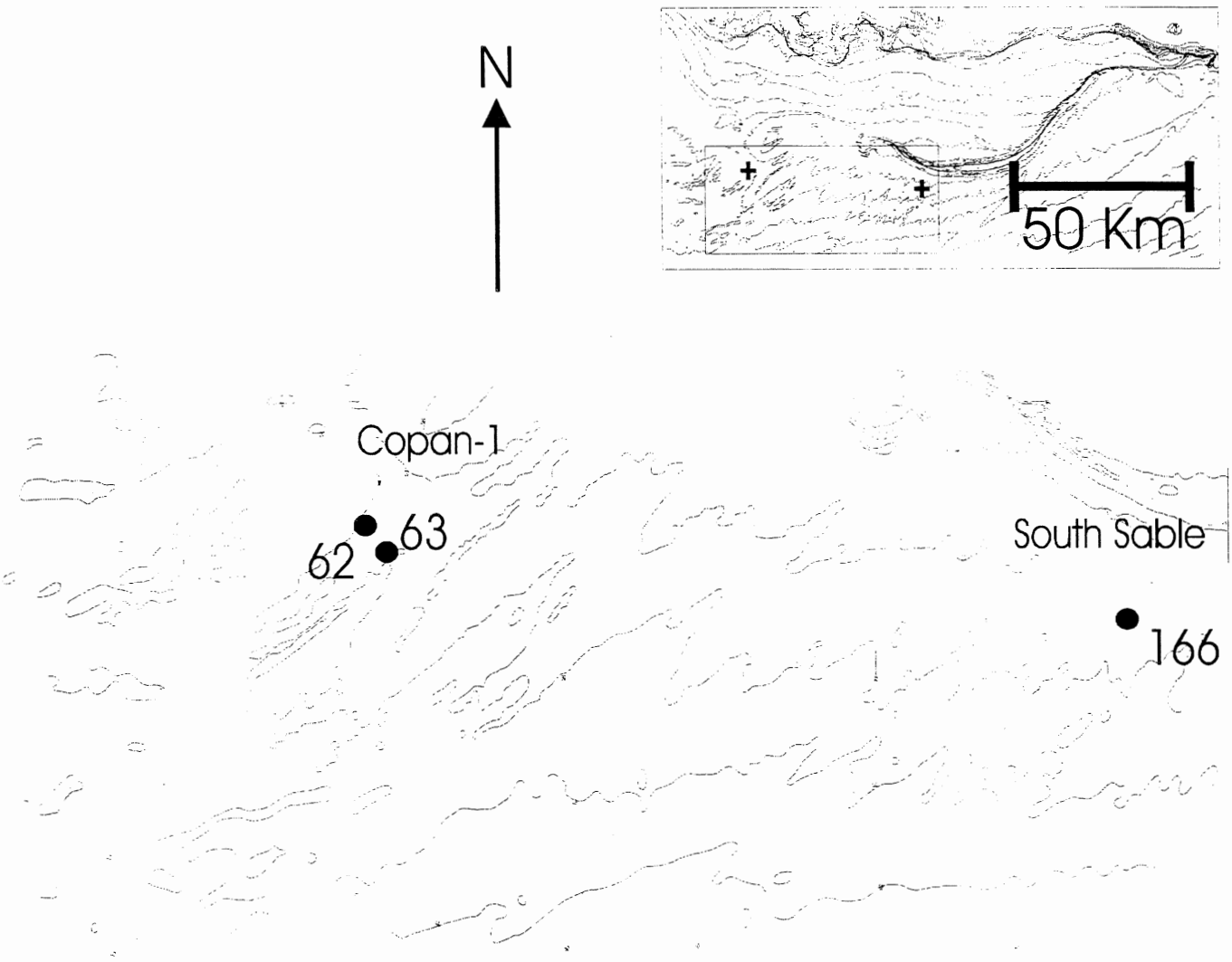

Figure 3.8 - Sampling locations on the Sable Island Bank for HUD-2000-30A samples (King, E., unpublished, 2001)

CHAPTER 4: DATA COLLECTION, ANALYSIS, AND RESULTS

4.1 Methods Used

The samples RAB-MB-1-6, (collected at Martinique Beach see chapter 3), were collected in daylight, and brought directly to the lab. Samples HUD-2000-30A-62, 63, and 166b, were collected from cores under subdued red light at the BIO and transported directly to the Dalhousie OSL laboratory. All work done on the samples was under subdued red light.

4.1.1 Water content Determination

The water content was determined on sub-samples (~15-20 g) placed in 1000 ml beakers and left uncovered overnight in an oven at ~60 °C. The samples were weighed before and after the drying process. Using the formula for water content determination (Δ_n),

$$\Delta_n = \frac{\text{(wet weight of sample – dry weight of sample)}}{\text{dry weight of sample}}$$

the water contents for the RAB-MB samples ranged from 0 to 0.28, 0 being RAB-MB-2 (the back dune) and 0.28 RAB-MB-1 (the lagoon).

Water content was not estimated for the HUD-2000-30A samples due to the samples being dried and sieved before it could be determined.

4.1.2 HCL Treatment

An HCL treatment was applied to the samples in order to rid the samples of any carbonates and to make sure that the samples were mostly composed of quartz. Mixed in the fume hood due to the effervescent nature of the reaction, a 50/50 solution composed of 36% HCl and distilled water was slowly added to the dried sand samples. This process was left to proceed to completion until there was no more reaction or bubbling. The samples were decanted and rinsed with four distilled water, two methanol, and two acetone rinses. Most samples showed little reaction with HCl as a result of the high content of quartz and few carbonates. Samples RAB-MB-5 and 6 effervesced vigorously. After rinsing, the samples were dried overnight in the oven at ~ 60 °C.

4.1.3 Sieving

Sieving allows the samples to be divided into specific grain sizes in order to facilitate sediment analysis and yield consistent results. The standard sieve sizes were used for the RAB-MB samples, 90, 125, 150, 180 and 354 μm (for RAB-MB-5 and 6).

The HUD-2000-30A samples were sieved before the HCl treatment and used, 63, 90, 125, 150,180, 210, and 250 μm, and 1 mm sieves. The sieving was done using a Haver & Boecker (1961) mechanical siever. The initial sieve was half filled with sample and put into the siever for 15 minutes at a time.

4.1.4 HF Treatment

The sieved samples were treated with 48% hydrofluoric acid (HF) using Nalgene beakers and stirring rods. Exercising extreme caution, about three times the sample volume of HF was added and left in the beaker for 40 minutes, stirring every 10 minutes. The beaker was then filled with 2/3 distilled water in order to stop the reaction. The solution was decanted into HF evaporation beakers in the fume hood. The samples were then rinsed four times with distilled water, twice with methanol and twice with acetone, and then placed in the oven to dry. This process etches the outside of the larger grains, and ensures that the smaller grains are removed.

4.1.5 Heavy Liquid Separation

A solution of 1,1,2,2-tetrabromoethane (TBE, specific gravity ~2.9) and methanol, MeOH, was prepared with the desired density of ~2.7. Using the simple formula:

[Desired Density (~2.7) x 100] – [ρMeOH x 100] = [(ρTBE – ρMeOH) x Vol of TBE required];
in which Vol of TBE required is being solved for

the exact amount of each chemical can be calculated. The solution was placed into a separatory funnel and the sample mixed in. Within about two hours, the lighter quartz grains were floating in the mixture, whereas the unwanted heavies were found at the bottom. This process was repeated with a desired S.G. of ~2.6, in order to float off unwanted feldspars which will float in a solution of this density. After the separation, the samples were rinsed with methanol to get rid of any TBE residue.

4.1.6 Magnetic Separation

Any magnetic grains in, by now, an almost purely quartz sample were removed by passing through a Frantz Isodynamic Separator. The samples were placed in a feeder-funnel, and left to separate over the course of about 6 hours.

4.1.7 Disk Preparation

Quartz grains, in allotments of ~5mg, were sprinkled onto the silicone spray-coated surface of each aluminum disc (measuring 1cm). For each sample, a specific number of disks was produced, ranging from 10-20. The discs were weighed and placed in light-tight containers and transported to the RISØ TL/OSL measurement room.

4.2 Optical dating protocols

As outlined in section 2, the measurement protocols developed for both multiple aliquot and single aliquot optical dating measurements include sequences of irradiation with calibrated laboratory doses, heating and, for quartz luminescence, stimulation with visible green light.

It is known (Aitken 1985, 1998) that natural quartz has charge traps at various energy levels (referred to as trap depths), and all of these participate in charge trapping processes during irradiation. Charges trapped in shallow traps are released very quickly, on time scales of minutes to years, and are therefore not relevant to the dating of geological deposits. In natural samples, therefore, the shallow traps are all empty since they have emptied naturally during their burial. In contrast, charges trapped in deep traps remain there indefinitely on a geologically relevant time scale (>1 million years). Since laboratory irradiation fills both shallow and deep traps, a procedure must be applied to release the charges from the shallow traps, so that the luminescence measured in both natural and laboratory-irradiated aliquots originates only from the deep, geologically relevant traps.

The procedure developed for this purpose is a preheat which follows irradiation and precedes the optical stimulation, and which involves heating to moderate temperatures of 220 to 240°C for brief periods of time (1 to 300s).

4.2.1 Preheating of very young samples

During the initial development of the multiple aliquot additive dose optical dating method, Godfrey-Smith (1991) observed an unexpected effect of the preheat on two modern samples to which she had applied the irradiation+preheat+stimulation protocol. In both instances, the natural, unheated aliquots yielded very low luminescence, and the growth of irradiated unheated samples was linear. In contrast, the natural preheated aliquots yielded a significantly higher luminescence, and the growth of irradiated preheated aliquots was initially supralinear (i.e., curving upwards), becoming linear only after a substantial dose was applied. Once the linear growth region was reached, the growth curves of unheated and preheated aliquots had the same slopes.

Godfrey-Smith (1991) was able to explain this behaviour as a thermal transfer due to the preheat, of charges from optically insensitive traps (TL traps not emptied by exposure to natural light) to optically sensitive traps. In addition, numerical modelling demonstrated that this thermal transfer process results in a very large luminescence signal if the optically sensitive traps are all initially empty, but not if at least some of these traps are initially filled.

If one is to date very young samples accurately, two things must be accomplished. First, the generation of a preheat-induced signal must be generalized, i.e., observed unequivocally in several samples. Secondly, an approach must be invented which circumvents the thermal transfer process. To this end, a preheat test experiment was developed, as follows:

Preheat Test Protocol:

1. Up to 14 aliquots of the quartz extracts of samples MB1 to MB5, Hud60 and Hud166, were prepared.
2. Half of these aliquots were first heated to 230°C for 300s
3. The luminescence of all aliquots was measured during stimulation for 250s
4. All aliquots were irradiated with 5 grays from a ^{90}Sr beta source.
5. All aliquots were heated to 230°C for 300s.
6. The luminescence of all aliquots was measured during stimulation for 250s.

4.2.2 Martinique Beach Optical Dating Protocol:

The natural growth curve protocol for the single aliquot analysis was as follows:

1. 15 aliquots were prepared, each consisting of ~5mg of quartz extract on a 1-cm Al disk
2. A radiation dose was applied to each aliquot
3. Each aliquot was preheated to 230°C for 300s
4. Each aliquot was stimulated with green light for 0.5s at 120°C, and its luminescence measured.
5. Steps 2 to 4 were repeated with different radiation doses for a total of 10 dose+preheat+shine cycles.

The incremental radiation doses applied in step 2 of each cycle were 0, 2, 2, 2, 2, 2, 2, 0, 0, 0 Gy, so that the total doses with which growth curves were constructed were 0, 2, 4, 6, 8, 10, 12, 12, 12 Gy.

Following the completion of the above mesurement, a preheat calibration run was carried out on the same 15 aliquots, with its protocol as follows:

1. Each aliquot was preheated to 230°C for 300s
2. Each aliquot was stimulated with green light for 0.5s at 120°C, and its luminescence measured.

The preheat calibration data were used to correct the growth curve data for signal depletion due to step 4 (the 0.5s stimulation) in each cycle.

The growth curve plus preheat calibration protocols were developed and tested using quartz which was annealed and given a laboratory dose of 4.4 Gy. Based on 10 single aliquot analyses, an average De = 4.46 ± 0.30 Gy was obtained, confirming that the protocols yield the expected dose (Godfrey-Smith, personal comm.).

The predose growth curve protocol was identical to the natural growth curve protocol as above, except that an irradiation of 3 Gy was given to each aliquot in step 2 of the first cycle, so that the total doses with which growth curves were constructed were 3, 5, 7, 9, 11, 13, 15, 15, 15 Gy. The preheat calibration run did not differ from that stated above.

4.3 Luminescence Data

4.3.1. Preheat Test results

Examples of the average first shine luminescence curves for 10 unheated and 10 preheated aliquots are shown below, for samples RAB-MB3 and Hud166.

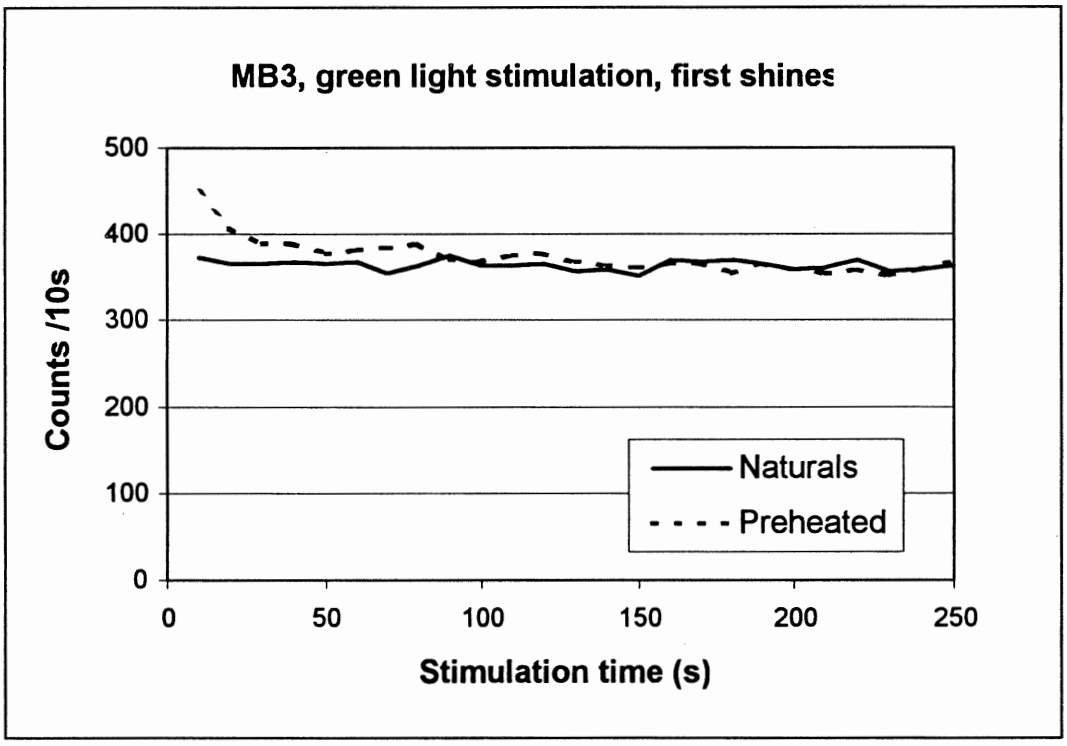

Figure 4.1 – Preheat test results for first shine, green light stimulation of RAB-MB-3

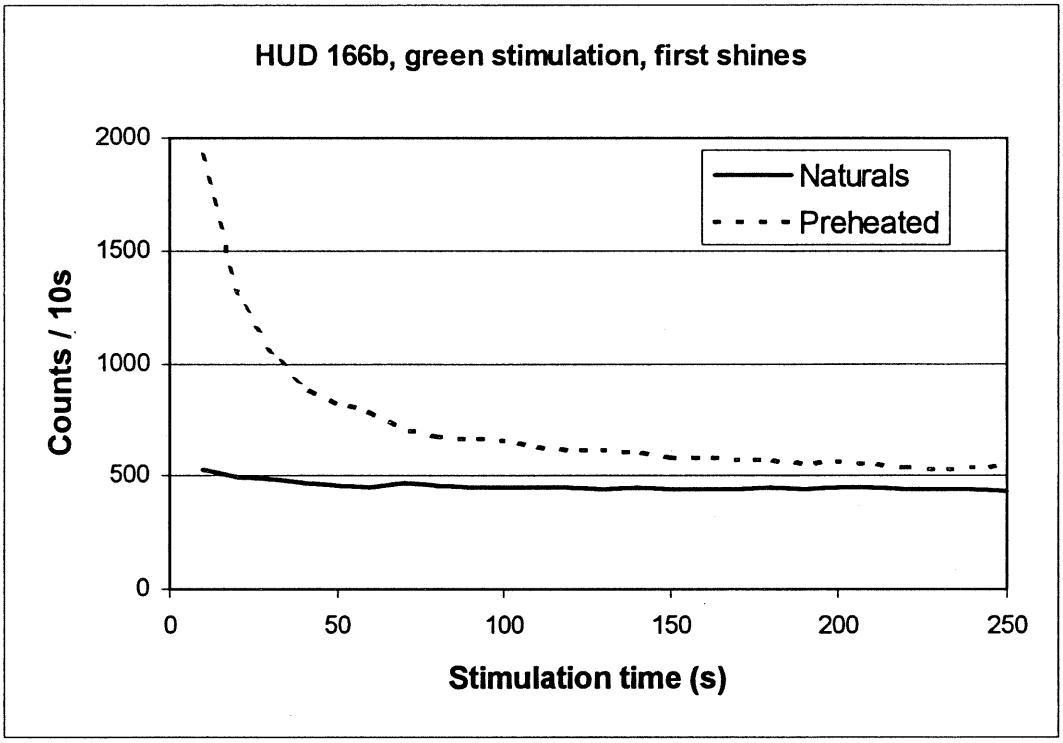

Figure 4.2 – Preheat test results for first shine, green light stimulation of HUD-2000-30A-166b

Both sets of curves show that the unheated luminescence (solid lines) is initially only slightly higher than the background values observed after 150s of stimulation. In contrast, the curves for preheated aliquots are initially higher. For the sake of brevity, similar graphs for the other Martinique Beach and Hudson core samples are not shown, but all showed identical behaviour.

The first and second shine data for all of these these measurements were analysed as follows:

The initial assumption is that the initial luminescence is due to charges from the most optically sensitive traps, and that the luminescence emitted after 100 or 200s of stimulation is due to charges in less optically sensitive traps. The shape of the

luminescence curve shows an initial peak followed by a rapid leveling off, and little if any change in the signal after about 150s of stimulation. The background value for each curve was therefore taken to be the 2-second average of the luminescence emitted during 200 to 220s of stimulation. The relevant initial luminescence emitted in Preheat Test Protocol steps 3 and 6 was taken as the first 2s of emitted luminescence, self background as defined above subtracted. The advantage of this approach is that this detects the net signal from the most light sensitive traps only, plus it also compensates for two sources of background noise: short-period variations in the photomultiplier detector's dark count due to environmental temperature and moisture variations, and the detected low levels of stimulating light scattered by the individual quartz grains on each aliquot.

An estimate of an average apparent residual De for each sample was obtained from the following calculation:

$$De = (\text{net first shine})/(\text{net second shine}) * 5\ Gy$$

The data in the table below are the averages of 4 to 14 individual aliquots. For samples MB5, Hud62, and Hud166, an apparent average De based on the first 10s net luminescence of 10 aliquots is also shown for comparison.

Sample	Unheated De (Gy)	Preheated De (Gy)	Preheat-induced dose (Gy)
RAB-MB1	0.59	1.21	0.62
RAB-MB2	0.16	3.18	3.02
RAB-MB3	0.21	0.90	0.69
RAB-MB4	0.05	0.84	0.79
RAB-MB5, 2 s	0.00	1.43	1.43
10 s	0.28	0.74	0.46
Hud62, 2 s	1.70	3.26	1.56
10 s	1.91	3.29	1.38
Hud166, 2s	0.094	1.07	0.98
10s	0.085	1.15	1.07

Table 4.1 – Preheat test results summarized for all samples

This result generalizes the original observation of Godfrey-Smith (1991) that the luminescence of a modern sample is naturally very near background, but that the laboratory procedure creates a much higher luminescence signal. The preheat-induced dose varies, but it can be as high as 3 Gy.

The predose growth curve protocol was developed following the completion of this data set. The rationale for pre-dosing the sample with such a substantial dose (which is equivalent to about 1000 years of post-depositional burial) is that this prevents the thermal transfer process from creating an unduly large artificial signal in a sample in which all optically sensitive traps are initially zero. In addition, it was expected that the growth of a predosed sample will be linear over the entire range of the growth curve rather than initially supralinear.

4.4 Single Aliquot Luminescence Data

All data were transferred from the RISØ machine into the Excel computer spreadsheet in order to manipulate the data and produce graphs.

Due to time constraints, RAB-MB-1 was the only sample to be processed for an equivalent dose (De). Two runs were made for this sample, the first was allowed to proceed naturally through the stimulation process, and the second was given an initial laboratory dose of 3 Gy of beta radiation. The addition of the beta radiation is intended to avoid a preheat-induced signal, which is generated in samples with zero, or nearly zero, optical signal. Adding 3 Gy of beta radiation should give a De just slightly higher than 3 Gy, because the preheat induced signal will not be generated with 3 Gy dose. The resultant De's for both methods are summarized in Table 4.1 and are the averages of the De's of all 15 disks.

Sample Number	De (Gy)
RAB-MB-1-a (Natural)	2.053 ± 0.308
RAB-MB-1-b (+3 Gy Beta Radiation)	0.430 ± 0.571

Table 4.2 – Summary of the De values for RAB-MB-1-a and RAB-MB-1-b

Figures 4.3 and 4.4 summarize the data graphically.

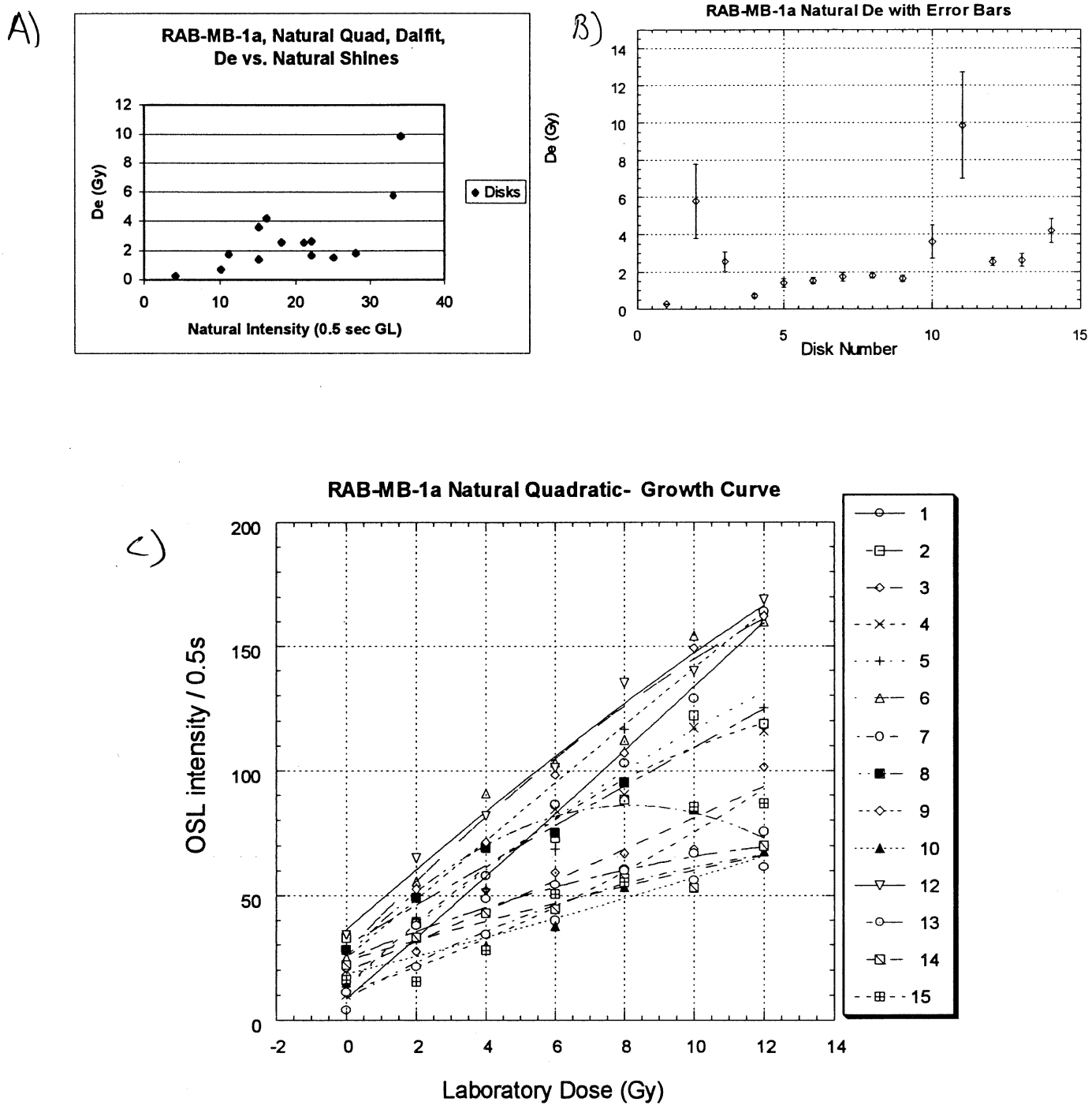

Figure 4.3 – Natural graphs for RAB-MB-1a. A) De versus Shines for 0.5 seconds of exposure to green light for 15 disks, excluding disk 11. B) The De's and their standard deviations are plotted for each disk, except 15. C) Growth curves for all of the disks, excluding 11.

A)

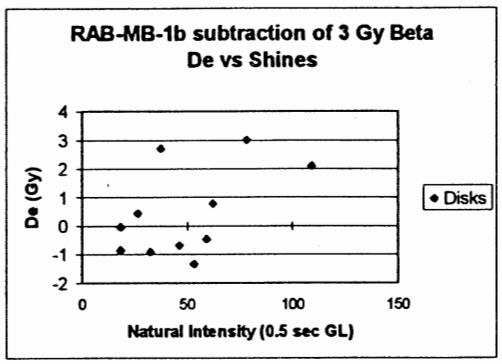

B)

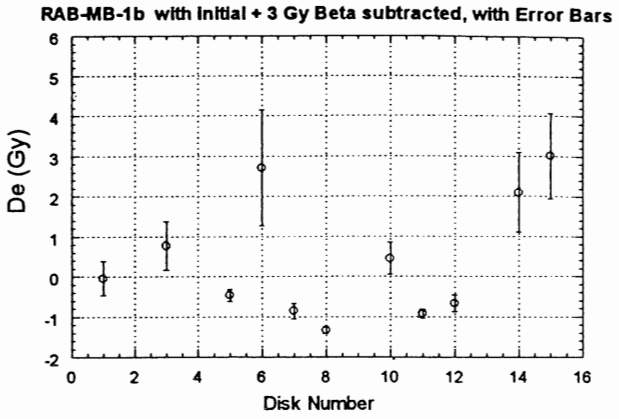

C)

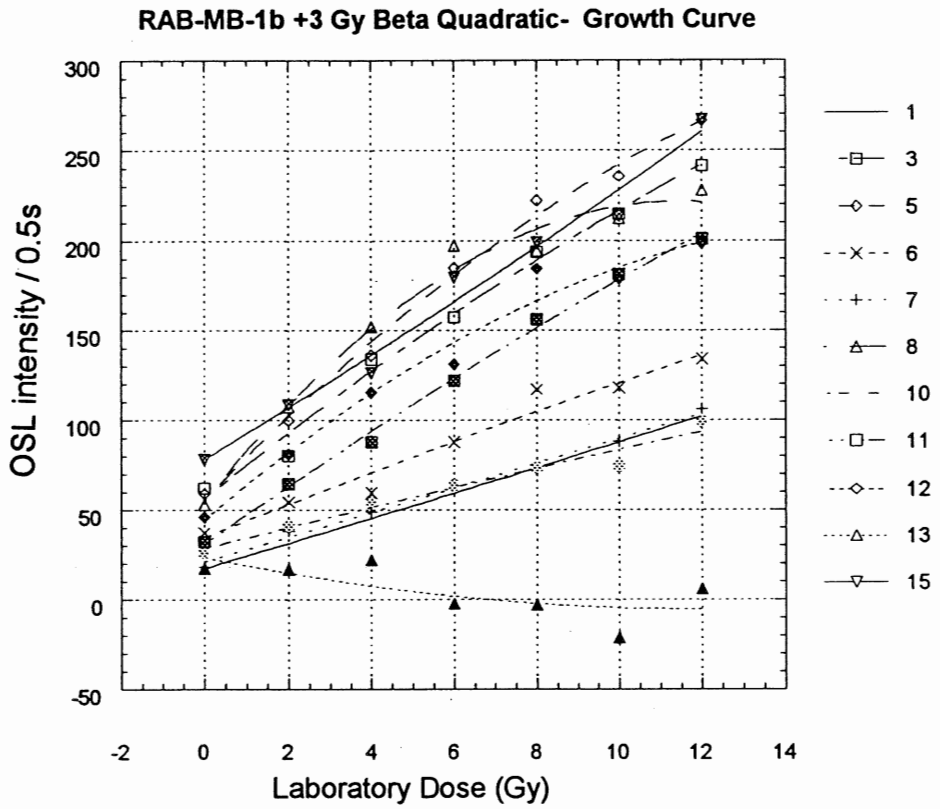

Figure 4.4 – Graphs with initial +3 Gy of Beta radiation for RAB-MB-1b. A) De, with initial 3 Gy subtracted, versus Shines for 0.5 seconds of exposure to green light for 15 disks, excluding disks 2, 4, 9 and 13. B) The De's, with initial 3 Gy subtracted, and their standard deviations are plotted for each disk, except 2, 4, 9 and 13. C) Growth curves for all of the disks, excluding 2, 4,9 and 14.

4.4.1 Graphs

The graphs observed in Figure 4.1 are representative of the natural protocol for RAB-MB-1a. The De's are a result of GL shining at specific laboratory doses in Gy for the span of 0.5 seconds. In graph A in Figure 4.1 the De's are plotted against natural intensity after exposure to 0.5 seconds of GL. The data points are broadly clustered with most points falling between 0 to 4 Gy and 4 to 30 natural intensity. There are two major outliers in this plot, one slightly below 6 Gy and the other slightly below 10 Gy. These may be indicative of grains that have not been completely bleached. These samples are also affected by a preheat-induced signal which may be causing the broad range in De's.

Graph B in Figure 4.1 gives the De and its standard deviation for the specific disks. The two main outliers can be clearly observed and pinpointed to disks 2 and 11. Graphs A and B help to identify the fact that the data for RAB-MB-1a are variable with much error.

Graph C in Figure 4.1 displays the growth curves for all of the disks, excluding disk 11. The curves display a wide range of forms ranging from linear to quadratic in nature. Extrapolating each curve to the x-axis, yields their De value which is then averaged to give the working De value.

The RAB-MB-1b graphs in Figure 4.2 are more representative of the young sample. RAB-MB-1b is the same sample as RAB-MB-1a, except for the initial 3 Gy of beta

radiation added at the beginning to overcome the preheat-induced signal which raises the overall De values.

Graph A in Figure 4.2 displays the De values against their natural shines (+3 Gy Beta). The 3 Gy of Beta have been subtracted from all of the De values giving an average De hovering around 0 Gy in a tighter cluster than in Figure 4.1-A. There are three outlier points above 2 Gy that may indicate incomplete bleaching.

Graph B in Figure 4.2 plots the De's of the disks with their standard deviations. There appears to be a larger standard deviation than sample RAB-MB-1a, with more outliers present.

Graph C in Figure 4.2 displays the growth curves for all of the disks with 3 Gy of beta radiation added, excluding disks 2, 4, 9 and 14. The data appear to be more quadratic than Figure 4.1-C. Disk 13 is a definite outlier. The extrapolated and averaged De value from 4.2-C is larger than from 4.1-C. This is corrected by subtracting the initial 3 Gy dose, yielding a much smaller De value.

4.5 Alpha Counting and Dose Rate Results

The dose rate of a sample (mentioned in section 2.1) is a product of exposure to radiation. The main radioactive isotopes are ^{40}K, natural U, and ^{232}Th from which alpha, beta and gamma particles are emitted.

Alpha counting is done using a three-bank Daybreak alpha counter. The sample was run for a total of eight days. The first four days were in an unsealed state and the last four were sealed. These counts are put into a ratio where the value ranges from 0 to 1, where values close to 1 indicate that no radon, ^{222}Rn, is escaping from the sample.

In order to obtain the dose rate from the alpha counting data, three specific values are needed: a) the total counts (C_{tot}), consisting of uranium and thorium values; b) the counts of thorium (C_{Th}); and c) the sealed/unsealed ratio.

The alpha counting results for samples RAB-MB-1 through 6 are summarized in Table 4.3. Due to lack of time, the HUD-2000-30A samples did not undergo alpha counting.

Sample Number	Unsealed Counting		Sealed Counting		Sealed to Unsealed ratio
	C_{tot}	C_{Th}	C_{tot}	C_{Th}	
RAB-MB-1	0.494 ± 0.008	0.208 ± 0.025	0.608 ± 0.011	0.237 ± 0.033	1.231
RAB-MB-2	0.194 ± 0.005	0.032 ± 0.010	0.197 ± 0.006	0.044 ± 0.014	1.012
RAB-MB-3	0.177 ± 0.006	0.083 ± 0.019	0.188 ± 0.006	0.069 ± 0.016	1.058
RAB-MB-4	1.192 ± 0.015	0.489 ± 0.051	1.179 ± 0.014	0.369 ± 0.043	0.989
RAB-MB-5	0.648 ± 0.011	0.210 ± 0.032	0.631 ± 0.010	0.210 ± 0.030	0.974
RAB-MB-6	0.382 ± 0.009	0.181 ± 0.028	0.367 ± 0.008	0.194 ± 0.028	0.960

Table 4.3 – Alpha counting results for RAB-MB-1 through 6.

4.5.1 Dose Rate Variables

Variables needed to calculate the dose rate of a sample are the alpha counting data, K_20 content, water content, depth below surface and the average grain size. The MB samples are a mixture of quartz, feldspar, and silt, likely from a granitic source.

Although we don't have the samples' K2O values, we can estimate them based on other samples we have from other nearby samples. Analyses of 5 samples from Lismore, Nova Scotia, from Cape Jourimain, New Brunswick, and from Pointe Deroche, Prince Edward Island, indicate that the best K2O estimate is 1.72 % (Godfrey-Smith, personal comm.).

The depth of the sample is also used is also an important variable within the calculation. For the purposed of the dose rate calculation, for samples which might have been buried very quickly following zeroing, an average depth of 0.45 m was assumed. The samples which were collected at depths greater than 0.45 m were given their real values for the calculation. This allows the full sphere dose to be applied to all samples (eventually - when all samples are analysed) and to compare them more systematically. Otherwise, the surface samples have only ½ of the full sphere gamma dose, and an effective dose rate underestimate in relation to the buried ones.

Sample Number	Alpha Counting Data: Average of Unsealed and Sealed		Water Content, Δ_n	Depth Below Surface (m)	Average Grain Size (μm)
	C_{tot}	C_{th}			
RAB-MB-1	0.551 ± 0.010	0.223 ± 0.029	0.282	0.45	137.5
RAB-MB-2	0.196 ± 0.006	0.038 ± 0.012	0.001	0.45	137.5
RAB-MB-3	0.183 ± 0.006	0.076 ± 0.018	0.226	0.45	137.5
RAB-MB-4	1.186 ± 0.015	0.429 ± 0.047	0.134	0.45	137.5
RAB-MB-5	0.640 ± 0.011	0.21 ± 0.031	0.032	0.45	165.0
RAB-MB-6	0.375 ± 0.009	0.188 ± 0.028	0.195	0.75	165.0

Table 4.4 – Dose rate variables for samples RAB-MB-1 through 6.

4.5.2 Dose Rate Calculation

Using the formulae outlined below in sections 4.4.2.1 to 4.4.2.3, all values were entered into an Excel spreadsheet and the values for dose rate and ages were calculated. The dry dose rate is initially calculated, yielding a value that has not yet taken into consideration the radiation absorbing properties of water. The wet dose rates take water content into consideration.

4.5.2.1 Beta Dose Rate R_β

The beta dose rate, R_β, is calculated using the following formula:

$$R_\beta \text{ dry} = 0.96\{(\beta_k)(0.676)(\%K_20) + (\beta_u)(1.15)(C_{tot}-C_{Th})\} + (\beta_{Th})(0.769)(C_{Th})$$

The values for $\beta_{k,\,u,\,Th}$ (beta attenuation factors, which are grain size dependent) are taken from Aitken (1985)(Figure C3, Appendix C, page 260), tabulated originally from Mejdahl (1979).

$$R_\beta \text{ wet} = R_\beta \text{ dry} / (1 + 1.25\Delta_n)$$

where Δ_n is the water content.

4.5.2.2 Gamma Dose Rate R_γ

The gamma dose rate, R_γ, is calculated using the following formula:

$$R_\gamma \text{ dry} = \{(0.202)(\%K_20) + 0.8868(C_{tot}) + 0.513(C_{Th})\}(Abs_\gamma)$$

The Abs_γ value is the proportion of gamma radiation absorbed, and is less than 1 if the sample is less than 30 cm below the surface. A simple ratio was set to complete this calculation:

$$Abs_\gamma = (\text{depth of sample in metres})(1 / 0.3)$$

$$R_\gamma \text{ wet} = R_\gamma \text{ dry} / (1 + \Delta_n)$$

4.5.2.3 Cosmic Dose Rate R_c

The cosmic dose rate, R_c, is calculated using the following formula:

$$R_c \text{ dry} = 0.21\{e^{(-0.07(2d) + 0.0005(2d)\text{^}2)}\}$$

Where d is the depth of the sample in metres.

$$R_c \text{ wet} = R_c \text{ dry} / (1 + \Delta_n)$$

4.5.2.4 Total Dose Rate R

$$R_{total} = R_{\beta}\ wet + R_{\gamma}\ wet + R_{c}\ wet$$

4.5.3 Total Dose Rate Calculation

The total dose rate calculations for all RAB-MB samples are found in Table 4.4 below.

Sample Number	Total Dose Rate R (Gy/ka)
RAB-MB-1	2.02 ± 0.10
RAB-MB-2	1.97 ± 0.13
RAB-MB-3	1.55 ± 0.09
RAB-MB-4	3.37 ± 0.17
RAB-MB-5	2.71 ± 0.16
RAB-MB-6	1.88 ± 0.10

Table 4.5 – Total dose rate calculations for samples RAB-MB 1 through 6.

4.6 Age Calculation

The ages of the samples are calculated using the age equation found in section 2.1,

$$\text{Age} = \text{Equivalent Dose } (D_e) \,/\, \text{Dose Rate } (R).$$

Using the equation above, the results for RAB-MB-1, natural and +3 Gy beta radiation, are summarized in Table 4.5 below. Due to time constraints, the De's of the other samples were not available.

Sample Number	De (Gy)	De (Gy) (RAB-MB-1-b – 3 Gy beta)	Dose Rate (Gy/ka)	Age (ka)
RAB-MB-1-a Natural	2.053 ± 0.31	2.053 ± 0.31	2.02 ± 0.10	1.02 ± 0.16
RAB-MB-1-b +3 Gy beta	3.430 ± 0.57	0.430 ± 0.57	2.02 ± 0.10	0.21 ± 0.28

Table 4.6 – Age of RAB-MB-1 using 2 methods, natural and addition of 3 Gy beta radiation.

CHAPTER 5: DISCUSSION AND CONCLUSION

5.1 Discussion

The intended purpose of this thesis was to investigate the zeroing properties of quartz with respect to different modern depositional environments. Samples were collected from a lagoon, back dune, mid-beach (down to 80 cm in depth), front beach, and large migratory oceanic dunes. Unfortunately, due to time constraints (mentioned in Chapter 4), RAB-MB-1 was the only sample to be evaluated in terms of equivalent dose, De, and therefore able to yield an age value. The dose rate was calculated for all RAB-MB's, as this information was dependent on the alpha counting data; time constraints did not allow enough time to analyze the HUD-2000-30A samples.

Using the single-aliquot regenerative-dose protocol (Murray and Wintle, 2000) two De values for RAB-MB-1 were generated. The first batch, RAB-MB-1a, was given no initial laboratory irradiation (natural), and was stimulated according to the protocol outlined in section 4.2, yielding a De value of 2.053 $\pm$ 0.308 Gy. The second batch, RAB-MB-1b, was initially irradiated with 3 Gy of beta radiation, yielding a De of 3.430 $\pm$ 0.571 Gy. The extra 3 Gy dose was added in order to avoid the preheat-induced signal that is generated in samples with zero, or near zero, optical signal. Subtracting the initial 3 Gy dose yields a much lower and more accurate De of 0.430 $\pm$ 0.571 Gy.

The De for RAB-MB-1b supports this thesis by yielding a value of zero within the standard deviation of De value, leaving the author to believe that in the lagoonal environment quartz grains are capable of being zeroed. This is somewhat surprising, due to the relative inactivity of the lagoon setting. The grains are not strongly reworked after deposition, and are overlain with thick mud and organic material. In comparison with the other samples, the lagoon would appear to be the more unlikely candidate for yielding efficient zeroing results. This could lead the author to believe that it may be possible for light to penetrate the sediment in order to bleach the quartz grains. A comparison with De's from the other samples would have to be performed in order to fully understand how well the lagoonal setting can be zeroed.

With a De value (0.430 Gy) this small, the error appears to be substantially larger, giving an error greater than 100 percent. It is common for De standard deviations to be approximately 10-20 percent of the De value in samples that are much older (Quickert 1998).

The dose rates for all RAB-MB samples were calculated using the formulae outlined in section 4.4.2. The calculations are standard and straightforward, leaving little room for error. The age calculated for RAB-MB-1b (0.21 ± 0.28 ka), falls within the standard deviation of 100 percent, resulting in a potential zero age.

5.2 Errors

The margin for error in this thesis has proven to be in the order of 100 percent. There are many variables that play small yet vital roles in the acquisition of a precise De value and eventually age. Although the lab work was done systematically, the possibility of contamination exists. Errors in data manipulation can also occur. The bulk of the error stems from the fact that the ages of the sediments are so young, giving analytical answers that are relatively small compared to the usual older data, in the order of thousands of years. It should also be noted that exposure to sun and the ability for quartz grains to be zeroed may vary from grain to grain, seen from outliers on Figures 4.1 and 4.2.

One issue with the calculation and the lagoon sample, is the fact that the water content in the lagoon is quite high, affecting the overall calculation, and therefore increasing the calculated dose rate, which in turn affects the final age calculation.

The protocol that was used may also be in question. These are new techniques that are continually evolving and need to be further tested. If the other samples had been put through the protocol, there may be some comparison and protocol issues.

5.3 Conclusion

Through systematic calculations and careful lab work it has been proven that a zero or near zero age can be achieved for sediments deposited in a lagoon – a modern environment with only modest reworking after deposition. As seen in Tables 4.1 and 4.5, the protocol plays a large role in accuracy of De values and ages. OSL is still a very young dating method, and it is apparent that the data have an immense variability and inconsistency, as shown by outliers, large standard deviations and experimental protocols.

REFERENCES

Aitken, M.J. 1985. Themoluminescence Dating. Academic Press Inc. (London) LTD.

Aitken, M.J. 1998. An Introduction to Optical Dating. Oxford University Press, Oxford.

Berger, G. W. 1990. Effectiveness of Natural Zeroing of the Thermoluminescence in Sediments. Journal of Geophysical Research, **95**: 12,375-12,397.

Duxbury, A.C., and Duxbury, A.B. 1997. An Introduction to the World's Oceans, fifth ed. WCB/McGraw-Hill.

Godfrey-Smith, D.I. 1991. Optical dating of sediment extracts. PhD thesis, Simon Fraser University, Burnaby, British Columbia.

Huntley, D. J., Godfrey-Smith, D. I., and Thewalt, M. L. W. 1985. Optical dating of sediments. Nature, **313**: 105-107.

Huntley, D.J., and Lian, O.B. 1997. Determining when a sediment was last exposed to sunlight by optical dating. A review for the Geological Survey of Canada Bulletin on the Palliser Triangle research.

Mejdahl, V. 1979. Thermoluminescence dating: beta-dose attenuation in quartz grains. Archaeometry, **21**: 61-73.

Murray, A.S., and Olley, J.M. 1999. Determining Sedimentation Rates using Luminescence Dating. GeoResearch Forum, **5**: 121-144.

Murray, A. S., and Wintle, A. G. 2000. Luminescence dating of quartz using an improved single-aliquot regenerative-dose protocol. Radiation Measurements, **32**: 57-73.

Nichols, G. 1999. Sedimentology and Stratigraphy. Blackwell Science, London.

Prothero, D.R., Schwab, F. 1996. Sedimentary Geology: An Introduction to Sedimentary Rocks and Stratigraphy. W.H. Freeman and Company, New York.

Quickert, N. A. 1998. Optically and Thermally Stimulated Luminescence Dating and Sedimentological Study of Birimi, a Mulit-Component Archaeological Site in Ghana, Africa. Unpublished M.Sc. Thesis, Dalhousie University, 219 pp.